

KfK 3043
Februar 1981

**Effects of
Space-Dependent Kinetics
on the Predisassembly Phase
of a Loss-of-Flow
Hypothetical Accident
in a 2000 MW_e LMFBR**

L. Väth
Institut für Neutronenphysik und Reaktortechnik
Projekt Schneller Brüter

Kernforschungszentrum Karlsruhe

KERNFORSCHUNGSZENTRUM KARLSRUHE

Institut für Neutronenphysik und Reaktortechnik
Projekt Schneller Brüter

KfK 3043

Effects of Space-Dependent Kinetics on
the Predisassembly Phase of a Loss-of-Flow
Hypothetical Accident in a 2000 MW_e LMFBR

L. Väth

Kernforschungszentrum Karlsruhe GmbH, Karlsruhe

Als Manuskript vervielfältigt
Für diesen Bericht behalten wir uns alle Rechte vor

Kernforschungszentrum Karlsruhe GmbH
ISSN 0303-4003

Abstract

Two-dimensional and point kinetics simulations of the predisassembly phase of an unprotected loss-of-flow accident in a large fast homogeneous reactor with two enrichment zones are compared, employing a refined core representation and an up-to-date voiding model. Though differences are appreciable during part of the transient, the total energy released differs by only 10 %, with point kinetics remaining conservative. It is pointed out, that this result cannot be generalized for other types of reactors or transients, especially heterogeneous cores.

Die Auswirkung von ortsabhängiger Kinetik auf die Einleitungsphase eines hypothetischen Kühlmittelverluststörfalls in einem natriumgekühlten schnellen Brutreaktor mit 2000 MWe Leistung

Zusammenfassung

Eine zweidimensionale und eine Punktkinetik-Simulation der Einleitungsphase eines Kühlmittelverlustunfalls in einem großen schnellen homogenen Reaktor mit zwei Anreicherungs-zonen werden verglichen, wobei ein verfeinertes Kernmodell und ein modernes Siedemodell verwendet werden. Obgleich in einzelnen Abschnitten des Transienten merkliche Differenzen zu beobachten sind, ändert sich die gesamte freigesetzte Energie um nur 10 %, wobei die Ergebnisse der Punktkinetik konservativ bleiben. Es wird darauf hingewiesen, daß dieses Resultat nicht für andere Reaktortypen oder Transienten verallgemeinert werden kann, insbesondere nicht für heterogene Reaktoren.

Contents

1. Introduction
2. The code KINTIC-2
3. Results for an LOF transient
4. Conclusions

Literature

Tables

Figures

1. Introduction

When simulating operational transients, non-destructive incidents, or the initiating phase of hypothetical accidents in fast reactors, space-dependent neutronics are often not accounted for. There are, mainly, two reasons presumably justifying this assumption:

- Fast reactors have a comparably large neutron mean free path causing a much stronger spatial neutron coupling of regions than in thermal reactors. A looser coupling with more pronounced effects of space-dependent dynamics can be expected for very big homogeneous or for heterogeneous reactors only.

- Space-dependent dynamics are needed only, when strong localized material movements are involved. The most common movement for transients not leading to core disruption is that of control rods. In this case, the effect of space-dependent neutronics can be easily taken into account by replacing the usual reactivity coefficients derived from first order perturbation theory by more correct ones from, e.g., A_k -calculations^{/1,2/}. Such a technique usually works well for small cores and becomes too costly only when the additivity of reactivity effects for different local material displacements is lost. This effect, again, is most severe for large fast reactors.

The material movements associated with the predisassembly phase of hypothetical core disruptive accidents may be qualitatively different from control rod movements; e.g. voiding processes may involve much larger regions. Thus, they have to be investigated separately. There are only a few studies on the importance of space-dependent neutronics for the predisassembly phase involving realistic models:

- In 1970, Kessler^{/3/} published a comparison of two-dimensional (2D) and zero-dimensional (OD) simulations of a transient overpower (TOP) excursion in a 300 MW_e fast reactor. The ramp is initiated by fast control rod withdrawal, which is explicitly modeled in the two calculations. Since the point kinetics calculation is not corrected for the errors of first order perturbation theory in control rod representation, the ramps are 85 \$/s in the 2D and 71 \$/s in the OD simulation.

The striking differences thus serve primarily to illustrate the errors of the most simplistic point kinetics control rod representation. The magnitude of space-dependent effects due to fuel-coolant-interaction (FCI) in the later stages of the predisassembly phase cannot be deduced from the results.

- In 1971, Mills and Kastenberg^{/4/} published a comparison of 1D and OD simulations of a 50 \$/sec TOP case in a 100 MW_e fast reactor. The geometric and neutronic model employed was quite coarse, leading to a mitigation of space-dependent effects. A difference of energy produced till the end of the transient of 11 % was found.
- Vãth and Struwe^{/5/} compared a 2D and OD simulation of a 5 \$/sec TOP excursion in a 300 MW_e LMFBR. Since prompt criticality is reached shortly before the end of the predisassembly phase in this case, the difference of reactor power at start of disassembly is 40 %, but reactivity, ramp rate, and energy released differ by only 7 % or less.
- Bezella and Ott^{/6,7/} carried out a comparison of 2D and OD results for a rapid loss-of-flow (LOF) transient in a 1000 MW_e LMFBR. No big differences are observed until the onset of voiding. This result agrees with the one of Jackson and Kastenberg^{/1/}, who in a simulation of feedback effects before voiding found point kinetics to be adequate. After the onset of voiding, voiding rates are very high in Bezella's case due to the big liquid superheat of 200^oC used. Thus, the total core region is quickly voided, and the reactivity repeatedly exceeds prompt critical. As can be expected for such a case, the effects of space-dependent neutronics are quite pronounced; when the core is entirely voided, the differences amount to about 30 % for total energy generation, 40 % for the power level, and 50 % for fuel melt fraction. On the other hand, a realistic value of liquid superheat has in the meantime been proved to be nearly two orders of magnitude lower than that employed by Bezella. This leads to lower voiding rates and attainment of prompt criticality only at later stages of the predisassembly phase, if at all. Effects are thus probably smaller for the newer LOF-models. Nevertheless, the results by Bezella point out the need for a careful analysis and, if necessary, some kind of correction of the

reactivity coefficients employed by point kinetics. According to the authors, a correction yielding acceptable point kinetics results is possible for their case^{/7/}.

- Galati et al.^{/28/} studied several TOP and two LOF cases for a 1000 MW_e LMFBR, comparing 2D simulations and point kinetics. Since an FCI model is lacking in the code employed, the TOP cases were stopped at fuel pin failure. The results from the TOP cases, which were driven by either an unspecified ramp or control rod movement, confirm that errors are large only when a strong localized material movement is involved. The two LOF cases are characterized by a very slow flow-coast-down (2 resp. 10 min. till onset of voiding) followed by high voiding rates in the channels affected. As in Bezella's case, point kinetics prove to be adequate till the onset of voiding; afterwards, results diverge drastically. Galati's calculations suffer from the coarse geometric representation employed - 6 channels for the whole core region. This leads to an unrealistic coherent voiding of large core regions, which may entail an overestimation of differences. Nevertheless, the potential magnitude of effects is again demonstrated.

- In all examples cited so far, the error in point kinetics results from employing first order perturbation theory and can be corrected by using some more accurate technique of calculating reactivity coefficients. The need for using space-dependent kinetics arises for such cases only, when the techniques for correcting point kinetics coefficients become more cumbersome than an approximate space-dependent method. More severe cases of space-dependent problems arise, when either the precursor distribution or even the prompt flux is not able to immediately follow a material movement, or when there is an appreciable difference of prompt and delayed flux distribution. Up to now, no such cases have been found for transients with intact subassemblies. It should be noted in this context, that Sienicki and Abramson^{/8/} examined the effect of precursor movement for a disassembly case. They found no significant differences resulting from the assumption that precursors remain stationary where they are created till the birth of delayed neutrons, instead of moving them with the fuel.

The results published so far may be summarized as follows: No extremely large effects have been found for transients with intact subassemblies, if reactivity effects caused by control rod movement are adequately treated. Existing studies indicate the potential for effects reaching the same order of magnitude as those resulting from uncertainties in other models, e.g. voiding or FCI-models. No comprehensive studies exist, but in view of the many types of fast reactors and possible transients such an undertaking would be extremely cumbersome. Since effects are not necessarily negligible, one should dispose of some kind of space-dependent code in order to be able to determine the magnitude of effects and possible corrections to point kinetics.

In Karlsruhe, the two-dimensional code KINTIC was developed since 1970, and preliminary versions were operational since 1972^{/2/}. Operational transients and other transients excluding changes of phase could be simulated with these first versions already. A simulation of the predisassembly phase of hypothetical core disruptive transients became possible only after newer thermodynamics and material movement models were adapted from the code system CAPRI-2^{/9/}, a point kinetics code developed in Karlsruhe. This new version of KINTIC, called KINTIC-2, is available since 1977^{/10/}, but had to be refined for some time until production runs for big cases became feasible. The code has recently been used to study a benign case of gas entrainment in the core of a 2000 MW_e homogeneous fast breeder^{/11/} and the predisassembly phase of an LOF transient in the same core. The latter calculations will be reported here, but before, a short summary of code capabilities will be given.

2. The code KINTIC-2

Code options of KINTIC-2 have been described in detail repeatedly^{/10,11/} and therefore will only be sketched here for reasons of completeness. The flow of calculations is depicted in Figs. 1 - 3.

- Group constants and precursors.

A set of basic group constants including the precursor data is created by auxiliary programmes^{/12/} before starting KINTIC-2. Up to 26 energy groups and 6 precursor groups are possible. Transient changes of material composition may affect the macroscopic group constants not only via the number densities but also, optionally, via changing resonance self-shielding factors altering the microscopic group constants.

- Stationary calculations.

Different options for criticality search (variation of dimensions or material composition) are provided, and an iteration is performed for achieving consistency of stationary neutronics and thermodynamics. Exact criticality is enforced at the end of the stationary part by dividing the number of neutrons per fission by the final multiplication constant. Up to now, no initial subcriticality is provided for.

- Neutron kinetics.

For space-dependent kinetics, the normal or improved quasistatic methods^{/13/} or the adiabatic method may be applied. Time-dependent flux shapes are inter- and extrapolated in order to be able to make the intervals for their recalculation as big as possible. Point kinetics may be performed with either externally supplied reactivity tables, or by internally calculating the coefficients with first order perturbation theory based on the initial flux and adjoint.

- Thermodynamics and material movement.

Space-dependent thermohydraulics of the core are modeled with up to 30 representative channels, which may be axially subdivided into up to 30 zones. The channels may represent different radial positions, power to flow ratios, or burnup states. One-dimensional models are used for the channels, which consist of one fuel pin surrounded by its share of coolant and structure material. Heat transport is radial in fuel and

cladding by conduction and axial in the coolant by convection. Transient changes of pressure distribution in the coolant are modeled. Fuel pin behaviour is treated by BREDA-II^{/14/}, which takes into account burnup and fission gas effects in modeling stationary and transient deformation and failure. The multiple bubble slug ejection model BLOW3^{/15/} is used for simulating voiding. Fuel element slumping is treated in a simplified way^{/16/}, assuming that fuel and cladding slump coherently; no dispersive processes are considered. The FCI-model is similar to the Cho-Wright model^{/17/} with a more refined treatment of heat transfer from fuel to sodium in the two phase region^{/18,30/}; axial fuel movements are not simulated, and FCI in a partially voided channel cannot be treated. The primary coolant circuit outside the core is not modeled. Material data utilized are those of the system MAPLIB^{/19/} developed in Karlsruhe.

- Feedback.

Feedback takes into account the changes in density and volume fraction of fuel, cladding, coolant, and structure material, fuel temperature, and axial length of the fuel column. Data of different channels, e.g. representing different burnups on the same radial position, may be averaged for the neutronic part. The changes are either fed into the group constants or, for the option employing reactivity tables, used for directly calculating the change in reactivity.

- External perturbation.

The transient may be initiated by simulating the following time-dependent events: Decrease of coolant inlet pressure, movement of control rods or fuel elements, localized movements of fuel, cladding, coolant, or structure material, and a reactivity ramp of unspecified origin.

- Time steps and iteration.

The choice of the different time steps for calculating global power increase, thermodynamics, material movements, and spatial flux distributions (see Fig. 3) as well as the decision on necessary iterations are highly automated with a few parameters left to the user for controlling accuracy.

- Code Organization.

KINTIC-2 is integrated in the Karlsruhe code system KAPROS^{/20/} in a modular form, making extensive use of its utility routines. Codes used apart from the CAPRI-2 modules mentioned above are the multigroup diffusion code DIXY^{/21/} and an adapted version of the point kinetics code AIREK^{/22/}. A restart and a plotting option^{/23/} are available.

3. Results for an LOF transient

The results of the earlier studies discussed in the introduction indicate that, apart from control rod movement, the predisassembly phase of an LOF accident has more potential for exhibiting large spatial effects than that of a TOP accident, due to its longer phase of material movement. Control rod movements have been studied already with realistic models, but the LOF cases calculated so far are only a few and lacking in detail and refined modeling. It was therefore decided to apply KINTIC-2 to an LOF case, using a big reactor, for which space-dependent effects can be expected to be large, and allowing for a sufficient representation of incoherency effects.

A 2000 MW_e homogeneous fast breeder reactor core investigated earlier at KfK^{/24,25/} was chosen for the study. Active core radius is 2.15 m and height 1.20 m for this design, with a .40 m upper and lower axial and a .28 m radial blanket. The core has two enrichment zones. Half of the elements are replaced at the end of one reactor cycle. Thus the end-of-cycle core used for the studies contains 50 % elements with half and 50 % with full burnup. The control rods are withdrawn to the core-blanket interface, resulting in a power distribution which is approximately symmetric in axial and relatively flat in radial direction with a slight central peak. The geometric representation used in earlier studies^{/26,27/} was employed and is shown in Fig. 4. The 29 thermodynamics channels are chosen to represent different radial positions, burnup states, and power to flow ratios. For the neutronics calculations neighbouring channels were lumped together as indicated in Fig. 4, and reflector zones were taken into account.

The transient analysed is the predisassembly phase of a hypothetical LOF accident with shutdown failure. Time-dependent loss of pressure in the primary circuit reduces the coolant mass flow to 50 % normal at 3.5 s and to 26 % at 6.5s, the onset of voiding. The axial expansion of the fuel is assumed to be 50 % effective. Voiding is initiated at a sodium superheat of 3^oC, leading to a low voiding rate. The end of the predisassembly phase is postulated to be reached when the energy averaged fuel temperature in the hottest node exceeds 3250^oC.

Due to the models employed, which do not take into account processes favouring early fuel dispersal, the simulation is clearly not a best estimate of the accident sequence. On the other hand it is not fully pessimistic, since axial fuel expansion is considered.

Time-dependent reactivity and power during the predisassembly phase are shown in Figs. 5 and 6 for the 2D simulation. There is only a slight power rise in the pre-voiding phase due to the effect of decreasing sodium density and volume fraction, which is only partly compensated by the Doppler and fuel expansion effect. Voiding conditions are reached at the upper core edge for all channels experiencing early voiding, whereas initialization is at an axially slightly lower position for channels starting later. The voiding process is initially slow due to the low superheat and accelerates due to enhanced film evaporation only when the voiding front reaches down into the high power axial region (see Fig. 11). Thus, large scale voiding of the zones having a strong positive void reactivity takes place only late in the transient. Reactor power therefore continues to rise but slowly after the onset of voiding and grows rapidly only in the last few 100 ms of the predisassembly phase.

Though the results are very similar to those from earlier OD simulations^{/25/}, they are not fully comparable due mainly to changes made on the voiding model in the meantime. Therefore, the comparative point kinetics calculations were performed with KINTIC-2, employing the option, which internally calculates first order perturbation effects.

The main differences of 2D and OD simulation may be deduced from Table 1, which summarizes the most significant results, and from Figs. 7 and 8. No appreciable difference is observed in the pre-voiding phase, thus confirming the results by Bezella and Ott^{/6,7/} and Galati et al.^{/28/}. Time-dependent reactivity and power after onset of voiding are compared in Figs. 7 and 8. The main deviation of the OD simulation appears to be a 10 % lengthening of the voiding phase, which is due to the constant underprediction of reactivity by first order perturbation theory.

A closer inspection of the results yields a number of details. First, the time-dependent evolution of differences will be discussed:

- Changes of neutron spectrum, effective fraction of delayed neutrons, and neutron generation time.

Spectral changes can be observed only approximately, since the energy dependence is represented by 6 rather coarse groups. Tab. 2 shows a comparison of time-dependent spectra in two reactor zones, only one of which is voided during the transient. Spectral changes remain below 6 %, apart from the 6th group, which is of minor importance for this case. The changes appear to be localized in and near the regions experiencing voiding, whereas the other regions have lower distortions. They occur only late in the transient, as can be expected with large scale voiding starting at that time.

The changes of the effective fraction of delayed neutrons - 1.0 % - and of neutron generation time - 2.8 % - are negligible (see Tab. 1). The small time-dependent changes occurring in the point kinetics case are due to the point kinetics option employed, which calculates not only reactivity effects with first order perturbation theory, but neutron generation time and effective fraction of delayed neutrons as well. The small effect on these two numbers is due to the changing group constants and is normally neglected, when reactivity tables are employed.

- Changes of flux and power distribution.

Fig. 9 illustrates the axial flux shift in a radial position near the center, i.e. one experiencing early voiding, Fig. 10 the radial distortion at about 3/4 core height. The flux has been normalized to a maximum value of 1 in both figures. The axial flux shift is obviously not serious; it is caused by the axial expansion of the fuel column, which amounts to 1.5 cm at the end of the predisassembly phase, and by the effect of the slightly higher multiplication in the voided region. This effect is more pronounced for the radial distribution, as can be expected from the large radial dimensions and thus weaker radial coupling. The magnitude of the radial shift depends only weakly on axial height.

Tab. 3 shows the time-dependent fraction of power released in a few zones at different radial positions. The axial position of these zones corresponds approximately to that of the radial flux distribution from Fig. 10. The fraction of power is, of course, influenced not only by the spatial flux distortion but as well by the space-dependent spectral

shift, density variations and Doppler effect. Nevertheless, the radial flux shift is clearly the main effect influencing the distortion of the power distribution, which has a maximum value of 15 %. The main effect occurs within the last 250 ms of the transient.

- Voiding sequence and velocity of voiding.

There is only a slight effect of space-dependent simulation on the voiding process. Voiding starts at the same time and the same axial position in all channels except number 24 and 25. These channels start latest - 1 s after onset of the voiding phase, i.e. shortly before the end of the predisassembly phase - and experience a time delay of 50 ms in the point kinetics case.

The voiding process in individual channels is very similar for the 2D/OD simulations, as is obvious from a comparison of Figs. 11 - 14. Figs. 11 and 12 show 2D and OD time-dependent voiding for channel 3, the central channel starting first. Figs. 13 and 14 make the same comparison for channel 16 at the radial edge of core zone 1, which starts half-way through the voiding phase. The pictures are very similar with the voiding rate being a little lower for the point kinetics case in the last 200 ms of the transient. This as well as the later onset of voiding in channels 24 and 25 for the OD case is due to the slower power rise which, after a time delay needed for heat transfer through the fuel element, translates into lower temperatures at the surface of cladding.

In the point kinetics case, the voiding process in all channels is, of course, 100 ms longer due to the elongated predisassembly phase. This causes the main differences of the void distribution at end of predisassembly.

- Time dependent reactivity and power.

As was stated above, there is a systematic underprediction of reactivity by point kinetics, which ultimately adds up to an elongation of the predisassembly phase by about 100 ms. At the beginning of the voiding phase, the lower power is due directly to the lower reactivity. In the late stages, an indirect effect is added by the slightly lower voiding rate affecting large regions of positive void effect, which is caused by the cumulative effect of lower power production, as explained above.

Some more detail can be deduced from an analysis of reactivity in the time interval between 6.0 and 7.3 s shown in Fig. 15. Reactivity rises slowly till the onset of voiding, due to the combined effects of sodium dilution, material expansion, and Doppler effect. This slow rise is kept up at the beginning of the voiding phase, since the first bubbles are small and in a region of low void reactivity, and thus do not contribute a significant effect. Then, from about 6.85 to 7.20 s, the void reactivity starts to show clearly. The fluctuations exhibited during this phase are due to bubbles collapsing and newly forming, but the average behaviour can be approximated by a linear rise with steeper slope. The linear behaviour is certainly due to the void distribution of the case considered and need not be the same in other cases. After about 7.2 s, large scale voiding sets in in the innermost channels, and reactivity starts to grow more rapidly. The curves cannot be compared directly any more beyond this point, because 2D and OD void distributions start to diverge slightly. A comparison of the slopes before 7.2 s yields the error of the point kinetics representation: The combined reactivity effects during the pre-voiding phase are underestimated by 11 %, the voiding effects by about 23 %. The last number applies to the void distribution during the phase before 7.2 s, i.e. a combination of central zones with strong positive effect and core edge and blanket zones with low positive and negative effects. Since this combination of zones being voided remains the same during the later stages of voiding, the error can be expected to remain near 25 %.

On the whole, though slight differences can be observed during the whole transient, the main differences develop during the last 200 - 300 ms. Differences are reduced slightly by the feedback of power production on the voiding rate late in the transient. Before drawing conclusions, the end of pre-disassembly results must be compared:

- Void fractions.

Figs. 16 and 17 show the distribution of voided regions at end of pre-disassembly. In spite of the slightly lower voiding rate, the OD void fraction is larger due to the longer duration of the transient. A quantitative measure of this effect is given by the numbers for over all void fractions in core zones 1 and 2 in Tab. 1, which differ by 24 and 37 %, respectively.

- Power, reactivity, and ramp rate.

These values are gathered in Tab. 1. Total power is 45 % higher in the 2D case. Reactivity is slightly below prompt critical and differs insignificantly. The total ramp rate is very low; the more significant number for follow-on calculations, ramp rate excluding Doppler, is low, too, and is 14 % smaller in the 2D case. The absolute difference is smaller for this number than for the total rate because the 2D Doppler-ramp is steeper, i.e. more negative, due to the higher 2D power level; the already smaller 2D ramp without Doppler is thus decreased by a bigger amount than in the OD case.

- Energy released above nominal, energy in molten fuel.

These two numbers are compared in Tab. 1. Though the power level is higher in the 2D calculation, the energy released is less due to the shorter time interval for voiding. Therefore, the energy contents of molten fuel is lower in the 2D case, too. The difference of the two values is 14 and 31 %, respectively.

- Core melt fraction.

As can be expected from the results on energy, the melt fraction is 25 % lower for the 2D calculations.

The results for end of predisassembly are thus mixed. Power and reactivity are higher for the 2D case, ramp rates, energy contents, melt and void fractions are lower.

The effect of these differences on total energy released during the whole transient was estimated using the parametric studies done by Maschek^{/27/} for the disassembly phase of the LOF transient in the core studied here. A few auxiliary calculations with the disassembly code KADIS^{/29/} had to be added, mainly for estimating the effect of changing the power at start of disassembly. The energy released during disassembly is, for the point kinetics case,

- by about $.8 \cdot 10^3$ MJ bigger due to the different reactivity ramp rate;
- by about $.3 \cdot 10^3$ MJ smaller due to the different initial reactivity
- by about $.9 \cdot 10^3$ MJ smaller due to the different initial power level.

Compared to the total energy released during disassembly, which is about $6.6 \cdot 10^3$ MJ^{/27/}, the net difference of about $.4 \cdot 10^3$ MJ is small. Furthermore, if the energies released during predisassembly and disassembly are added (see Tab. 1), the OD estimate turns out to be 10 % higher than the 2D value. This difference is augmented by the effect of the lower 2D void fraction at start of disassembly, which has not been covered by the parametric studies. A lower void fraction acts to shorten the disassembly phase because of the higher Doppler constant associated, and because the material motion ending the transient is accelerated^{/27/}.

Another set of auxiliary calculations was performed in order to assess the magnitude of the point kinetics error resulting from underprediction of the sodium void reactivity alone. For this, stationary Δk -calculations were performed for different partly voided core configurations and compared to the results from first order perturbation theory (Table 4). These results must be compared with the error in reactivity increase at voiding deduced from Fig. 15 (see above), which amounts to 23 %. Two conclusions can be drawn:

- The result for voiding core zone 2 alone exceeds the actual error. Such a result can be expected, since the void distribution is very different from the one developing during the actual transient. Thus, if correction factors are derived from stationary calculations, care should be taken to use a void distribution typical for the transient.

- The results for void distributions approaching the actual one underestimate the effect. Other effects are responsible for the difference, mainly axial expansion and change of Doppler feedback in the deformed space and energy distribution of the neutron flux. Nevertheless, about half of the difference is caused by the sodium effect alone.

4. Conclusions

2D and OD simulations of the predisassembly phase of an unprotected LOF accident in a large LMFBR have been compared, and the change in energy released during the transient including the disassembly phase was estimated. The following conclusions can be drawn - all of them regarding, of course, only fast reactors:

- Though point kinetics results may differ markedly from those of the space-dependent simulation during part of the transient, the overall effect on energy released is only 10 %. The point kinetics estimate is conservative. One should keep in mind, however, that this result is valid for the type of reactor and transient treated here and cannot be easily generalized.
- The results found for different burn-up states or design modifications^{/25/} show deviations of the same order of magnitude or even bigger ones. Additional uncertainties result from the models describing material motions. Thus the effect of space-dependent neutronics is not of primary concern in this case.
- A comparison of stationary calculations of the void effect with first order perturbation theory on the one, and Δk -calculations on the other hand yields an estimate of the point kinetics error covering about half of the total deviation. Such an estimate is readily calculated and may be recommended for incorporation in a point kinetics calculation based on first order perturbation theory, since results are improved and, at the same time, remain conservative. Care should be taken to use a characteristic void distribution for deriving the correction.
- The usefulness of a space-dependent code has been demonstrated. Though KINTIC-2 is decidedly not suited for routine calculations, such a code may be needed from time to time for evaluating the importance of space-dependent effects.
- The space-dependent effects resulting from control rod motion can be readily corrected in point kinetics calculations by employing correct

worth curves. One may be tempted to deduce from the results presented, which involve a large core as well as large scale material movements, that other space-dependent effects may be neglected. This may not be valid generally, since transients in large heterogeneous reactors have not been simulated so far. The looser coupling of core regions in a heterogeneous core will probably enhance effects, which at 10 % of energy released for the homogeneous core are not totally negligible even here. In addition, point kinetics need not remain conservative. Therefore, space-dependent effects will have to be investigated in the course of safety studies for heterogeneous cores. The same is true for large homogeneous cores, if a significantly different design or type of transient is involved.

Acknowledgement

The author would like to thank M. Bottoni, R. Fröhlich, E. Kiefhaber, W. Maschek, and D. Struwe, all of KfK, for their help in adapting the CAPRI-2 modules, providing the input data, and for fruitful discussions, and Mrs. Bunz for typing the manuscript.

Literature

- /1/ J. F. Jackson, W. E. Kastenberg: "Space-Time Effects in Fast Reactor Dynamics"; Nucl. Sci. Eng. 42, 478 (1970)
- /2/ L. Mayer, H. Bachmann: "KINTIC-1: A program for the calculation of two-dimensional reactor dynamics of fast reactors with the quasi-static method"; KFK 1627 (1972)
- /3/ G. Kessler: "Space-dependent Dynamic Behavior of Fast Reactors Using the Time-Discontinuous Synthesis Method"; Nucl. Sci. Eng. 41, 115 (1970)
- /4/ J. C. Mills, W. E. Kastenberg: "An axial kinetics model for fast reactor disassembly accidents"; Conf 710302, p. 167 (1971)
- /5/ L. Vãth, D. Struwe: "Space time dependent codes and problems of few group cross section schemes"; TANSO 20, 554 (1975)
- /6/ W. A. Bezella: "A Two-Dimensional Fast Reactor Accident Analysis Model with Sodium Voiding Feedback Using the Synthesized Quasistatic Approach"; Purdue Univ., Lafayette, Ind., Diss. 1972
- /7/ W. A. Bezella, K. O. Ott: "Two-Dimensional Spatial Effects in Fast Reactors During Sodium Voiding"; TANSO 14, 737 (1971)
- /8/ J. J. Sienicki, P. B. Abramson: "Effects of recent modeling developments in prompt burst hypothetical core disruptive accident calculations"; Nucl. Technol. 40, 106 (1978)
- /9/ D. Struwe et al.: "CAPRI - A computer code for the analysis of hypothetical core disruptive accidents in the predisassembly phase"; CONF-740401, p. 1525 (1974)
- /10/ L. Vãth: "KINTIC-2 user's manual"; KFK 2508 (1977)

- /11/ L. Váth: "Ortsabhängige Simulation des Störfallverhaltens bei Schnellen Reaktoren mit dem Rechenprogramm KINTIC-2"; Atomkernenergie-Kerntechnik 35, 275 (1980)
- /12/ L. Váth: "Calculation of group constants for use in the two-dimensional dynamics code KINTIC-2"; KFK 2289 (1976)
- /13/ K. O. Ott, D. A. Meneley: "Accuracy of the quasistatic treatment of spatial reactor kinetics"; Nucl. Sci. Eng. 36, 402 (1969)
- /14/ B. Kuzcera: "Simulation of the transient behaviour of LMFBR fuel pin under consideration of special burnup phenomena using the BREDA-II model"; Nucl. Eng. Design 31, 294 (1974)
- /15/ P. Wirtz: "Ein Beitrag zur theoretischen Beschreibung des Siedens unter Störfallbedingungen in natriumgekühlten schnellen Reaktoren"; KFK 1859 (1973)
- /16/ G. Angerer: "Transport von Kernmaterialien während Unfällen in Schnellen Natriumgekühlten Brutreaktoren (Slumping)"; KFK 1935 (1974)
- /17/ D. H. Cho et al.: "Pressure Generation by Molten Fuel-Coolant Interaction under LMFBR Accident Conditions"; CONF 710302, p. 25 (1971)
- /18/ L. Caldarola: "A theoretical model for the molten fuel-coolant interaction in a nuclear fast reactor"; Nucl. Eng. Design 22, 175 (1972)
- /19/ U. Schumann: "MAPLIB - Ein Programmsystem zur Bereitstellung von Stoffdaten für Rechenprogramme"; KFK 1253 (1970)
- /20/ H. Bachmann, S. Kleinheins: "Kurzes KAPROS-Benutzerhandbuch"; KFK 2317 (1976)
- /21/ W. Höbel: "Numerical methods used in the two-dimensional neutron diffusion program DIXY"; Proc. of the GAMM-Workshop on fast solution methods for the discretized Poisson equation, Karlsruhe (1977)
- /22/ L. R. Blue, M. Hoffman: "AIREK3; Generalized Program for the Numerical Solution of Space Independent Reactor Kinetics Equations"; AMTD-131 (1963)

- /23/ W. Zimmerer: "PLOTCP - Ein Fortran IV-Programm zur Erzeugung von Calcomp-Plot-Zeichnungen"; KFK 2081 (1975)

- /24/ G. Heusener et al.: "Entwurfsstudien für das SNR-2 Core";
Atoomenergie 18, 211 (1976)

- /25/ D. Struwe et al.: "Safety Analysis Aspects of a 2000 MW_e LMFBR Core";
CONF 761001, Vol. I, p. 193 (1976)

- /26/ D. Struwe: "Das Verhalten des Kerns eines natriumgekühlten Schnellen
Brutreaktors von 2000 MW_e bei Störfällen sehr geringer Eintritts-
wahrscheinlichkeit"; KFK 2490 (1977)

- /27/ W. Maschek: "Analyse der Disassemblyphase schwerer hypothetischer
Störfälle für den SNR-2000"; KFK 2491 (1977)

- /28/ A. Galati et al.: "Neutron flux shape effects in large fast reactor
safety calculations"; CNEN-RT/FI (78) 20 (1978)

- /29/ P. Schmuck et al.: "KADIS: ein Computerprogramm zur Analyse der
Kernzerlegungsphase bei hypothetischen Störfällen in schnellen,
natriumgekühlten Brutreaktoren"; KFK 2497 (1977)

- /30/ E. A. Fischer, unpublished results.

State		2D results	OD results
Stationary	effective fraction of delayed neutrons	3.817-3	3.817-3
	neutron generation time(s)	4.71-7	4.71-7
Onset of voiding	time (s)	6.5	6.5
	normalized power	1.21	1.19
	reactivity (\$)	.0995	.0907
	effective fraction of delayed neutrons	3.824-3	3.817-3
	neutron generation time(s)	4.69-7	4.72-7
End of pre-disassembly	time (s)	7.5504	7.6471
	normalized power	410.	225.
	reactivity (\$)	.981	.975
	effective fraction of delayed neutrons	3.855-3	3.818-3
	neutron generation time(s)	4.58-7	4.76-7
	reactivity ramp (\$/s)		
	total	-4.9	.5
	without Doppler	17.8	20.3
	energy released above nominal power (MJ)	3.82+4	4.35+4
	energy contents of molten fuel (MJ)	6.26+3	8.22+3
	void fraction (%)		
	core 1	42.5	52.9
	core 2	14.8	20.3
core melt fraction (%)	29.3	36.6	

Table 1: Comparison of significant results for 2D and OD simulation of LOF transient in 2000 MW_e LMFBR

Position: Half core height, central (early voiding) channels

Group	Energy	t = 0 s	t = 6.5 s	t = 7.05 s	t = 7.325 s	t = 7.5504 s	Max. Deviat.
1	1.4 - 10.5 MeV	7.5 %	7.5 %	7.5 %	7.6 %	7.7 %	2.7 %
2	.4 - 1.4 MeV	17.2	17.3	17.3	17.4	18.1	5.2
3	46.5 - 400 keV	45.7	45.8	46.0	46.2	47.5	3.9
4	10.0 - 46.5 keV	20.0	19.9	19.8	19.7	18.9	-5.5
5	1.0 - 10.0 keV	6.0	6.0	6.0	5.9	5.9	-1.7
6	0 - 1.0 keV	3.6	3.5	3.4	3.2	1.9	-47.2

Position: Half core height, outer (late voiding) channels of core zone 1

Group	Energy	t = 0 s	t = 6.5 s	t = 7.05 s	t = 7.325 s	t = 7.5504 s	Max. Deviat.
1	1.4 - 10.5 MeV	7.3 %	7.3 %	7.3 %	7.3 %	7.3 %	0.0 %
2	.4 - 1.4 MeV	17.1	17.1	17.2	17.2	17.3	1.2
3	46.5 - 400 keV	45.4	45.6	45.6	45.6	46.0	1.3
4	10.0 - 46.5 keV	20.2	20.1	20.1	20.1	20.0	-1.0
5	1.0 - 10.0 keV	6.0	6.0	6.0	6.0	5.9	-1.7
6	0 - 1.0 keV	4.0	3.9	3.8	3.8	3.5	-12.5

Table 2: Spectral shifts in two core positions

Radial position of zone (cm)	8.7 - 31.3 (Core 1, middle)	131.4 - 141.4 (Core 1, edge)	211.9 - 215.0 (Core 2, edge)
Time (s)			
0.	1.27-3	3.35-3	.84-3
6.5	1.28-3	3.35-3	.84-3
7.05	1.28-3	3.33-3	.84-3
7.325	1.32-3	3.32-3	.83-3
7.5504	1.46-3	3.29-3	.80-3
Maximum deviation (%)	15	2	5

Table 3: Time-dependent fraction of power released in zones at different radial positions (axial height: 125.7 - 131.4 cm)

Case	Voided zone	Δk -calculation	first order perturbation	Error
1	Core zone 2	.34 \$.21 \$	38 %
2	Upper .66m of core zone 1	3.38 \$	2.99 \$	11.5 %
3	As case 2, but in addition first radial .13 m of core zone 2 and axial blanket above voided core zones	3.37 \$	2.95 \$	12.5 %

Table 4: Comparison of void reactivities derived from stationary Δk -calculations and from first order perturbation theory

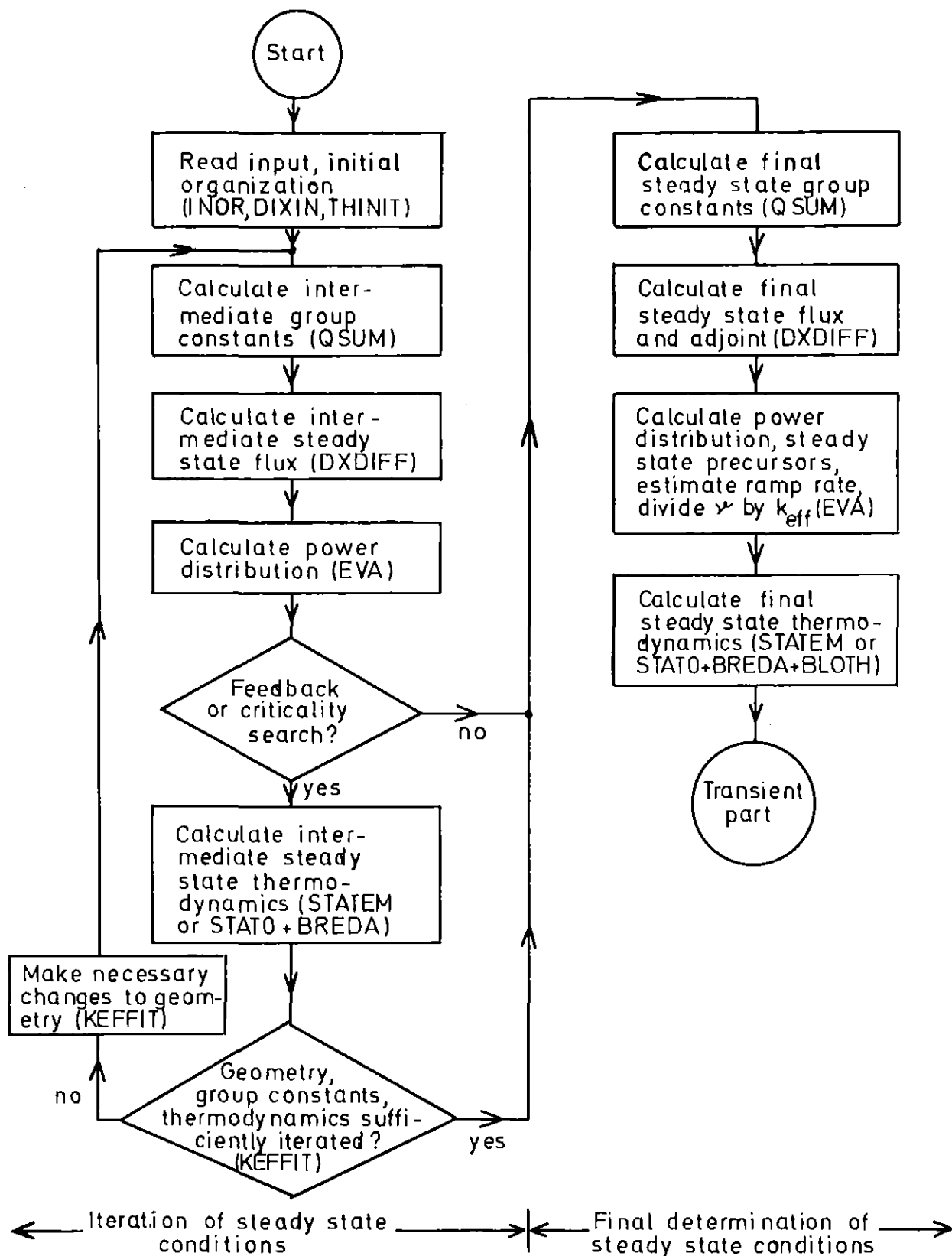


Fig. 1: Flow chart of steady state part of KINTIC-2

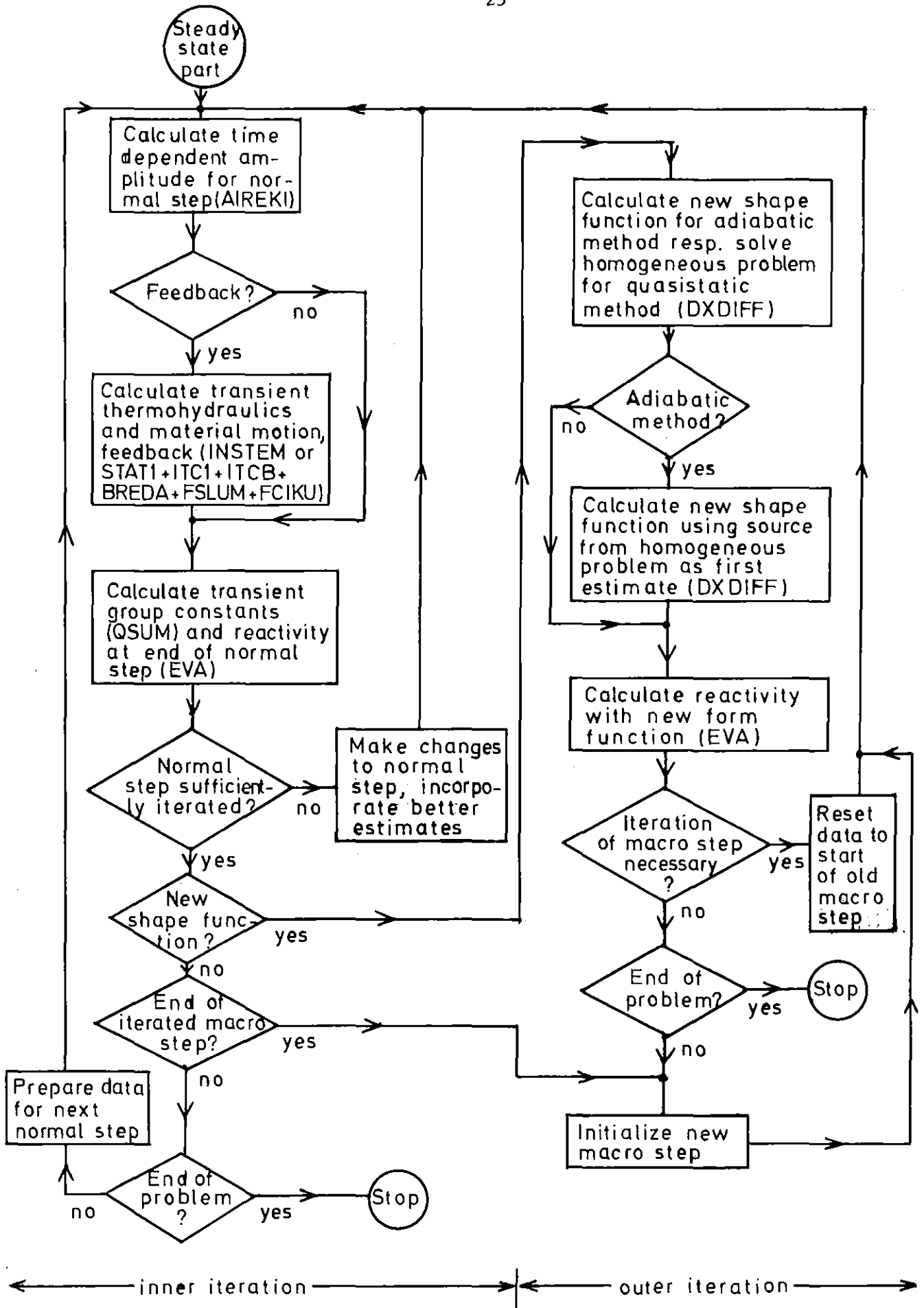


Fig. 2: Flow chart of transient part of KINTIC-2

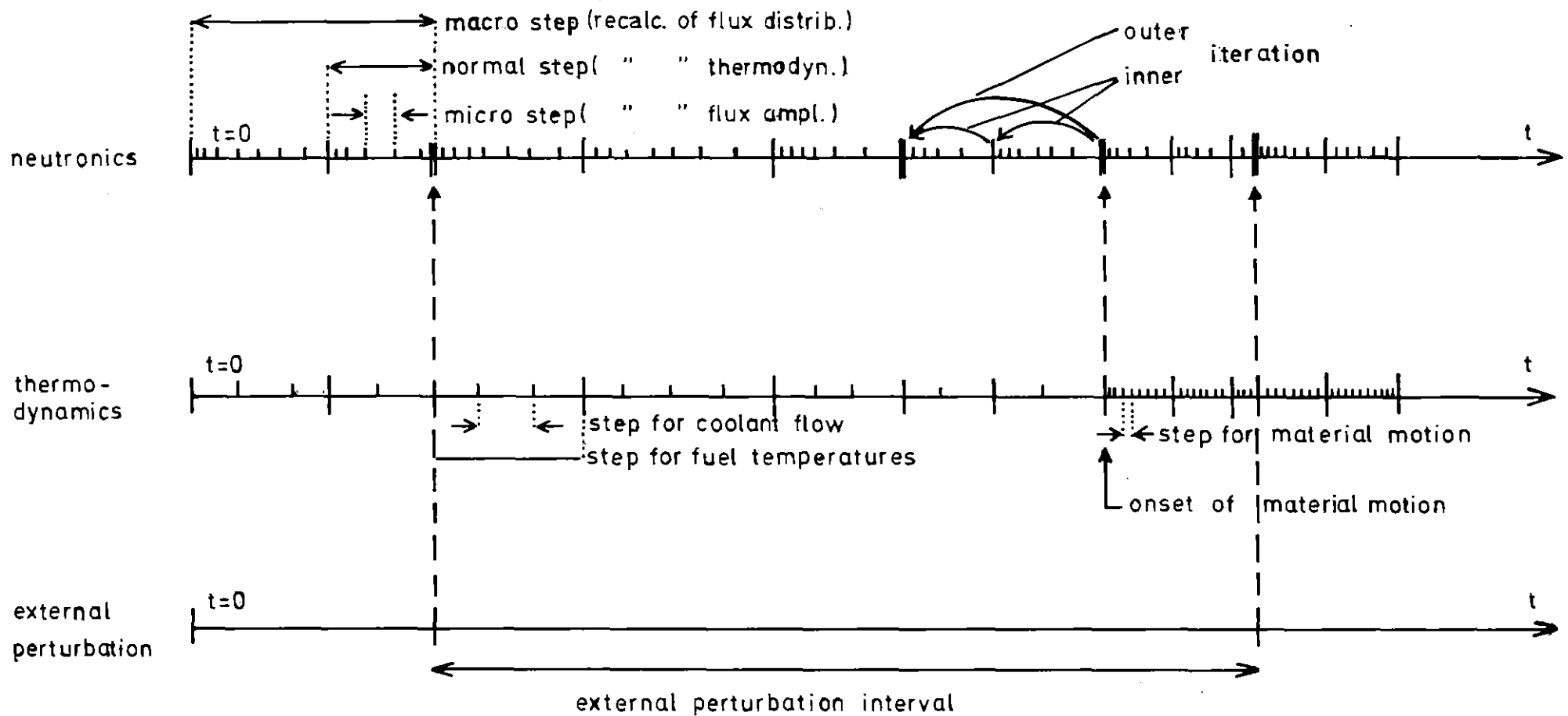


Fig. 3: Interaction of time scales in KINTIC-2

- | | | | |
|---|------------------------|---|----------------------------------|
| — | end of normal interval | — | end of micro interval or end of |
| — | end of macro interval | | internal thermodynamics interval |

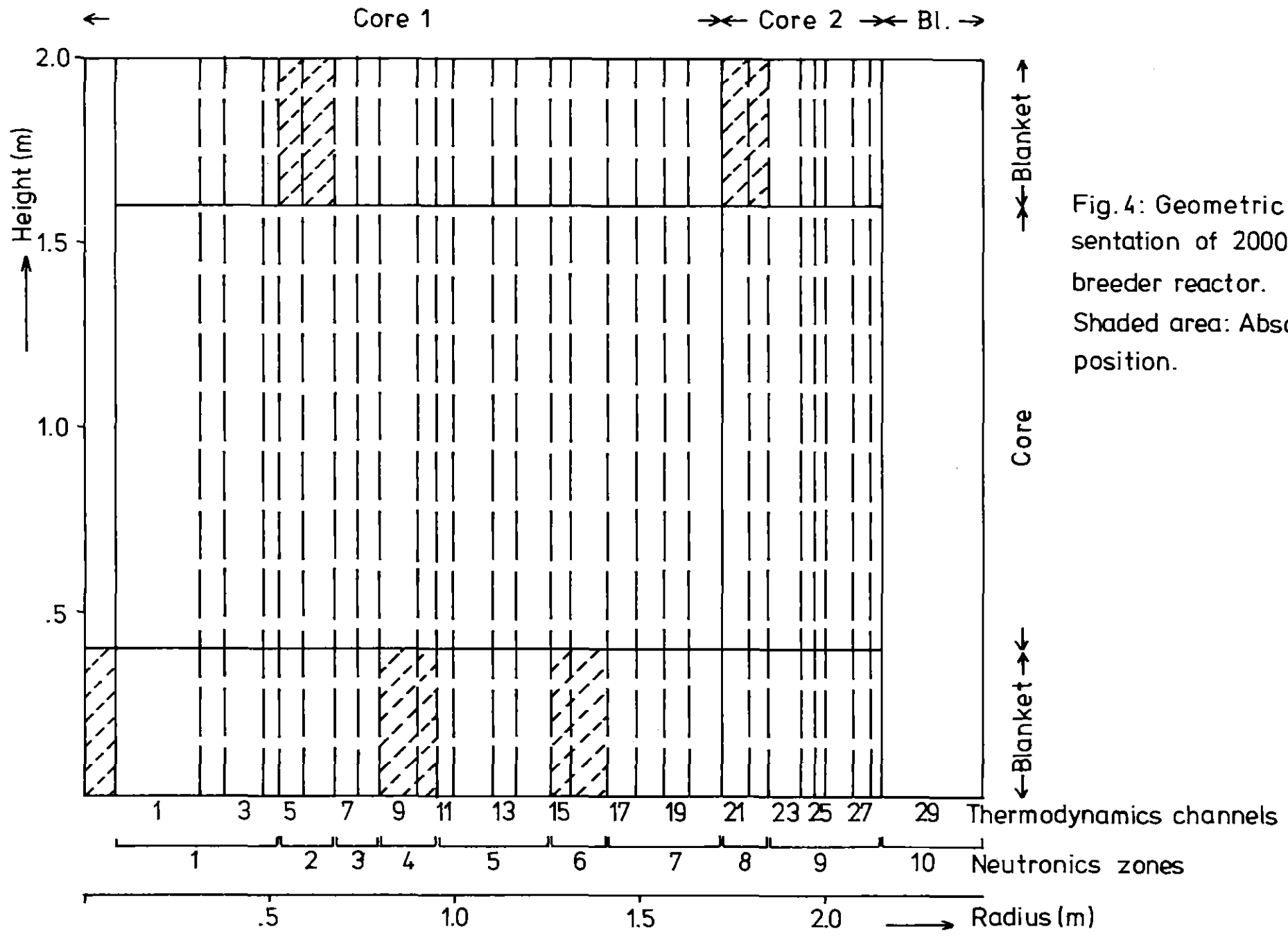


Fig.4: Geometric representation of 2000 MWe breeder reactor. Shaded area: Absorber position.

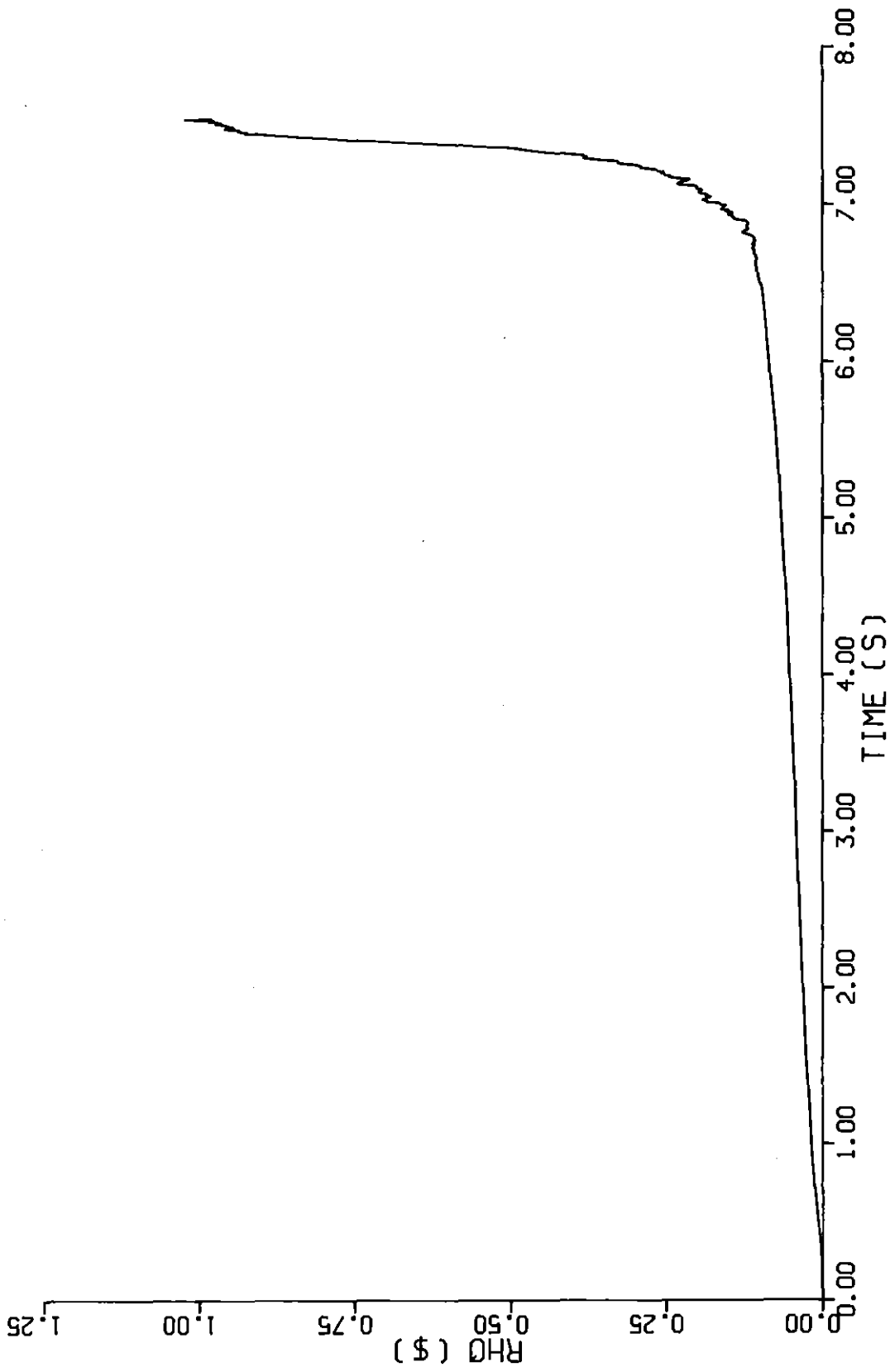


FIG. 5: TIME DEPENDENT REACTIVITY (2D)

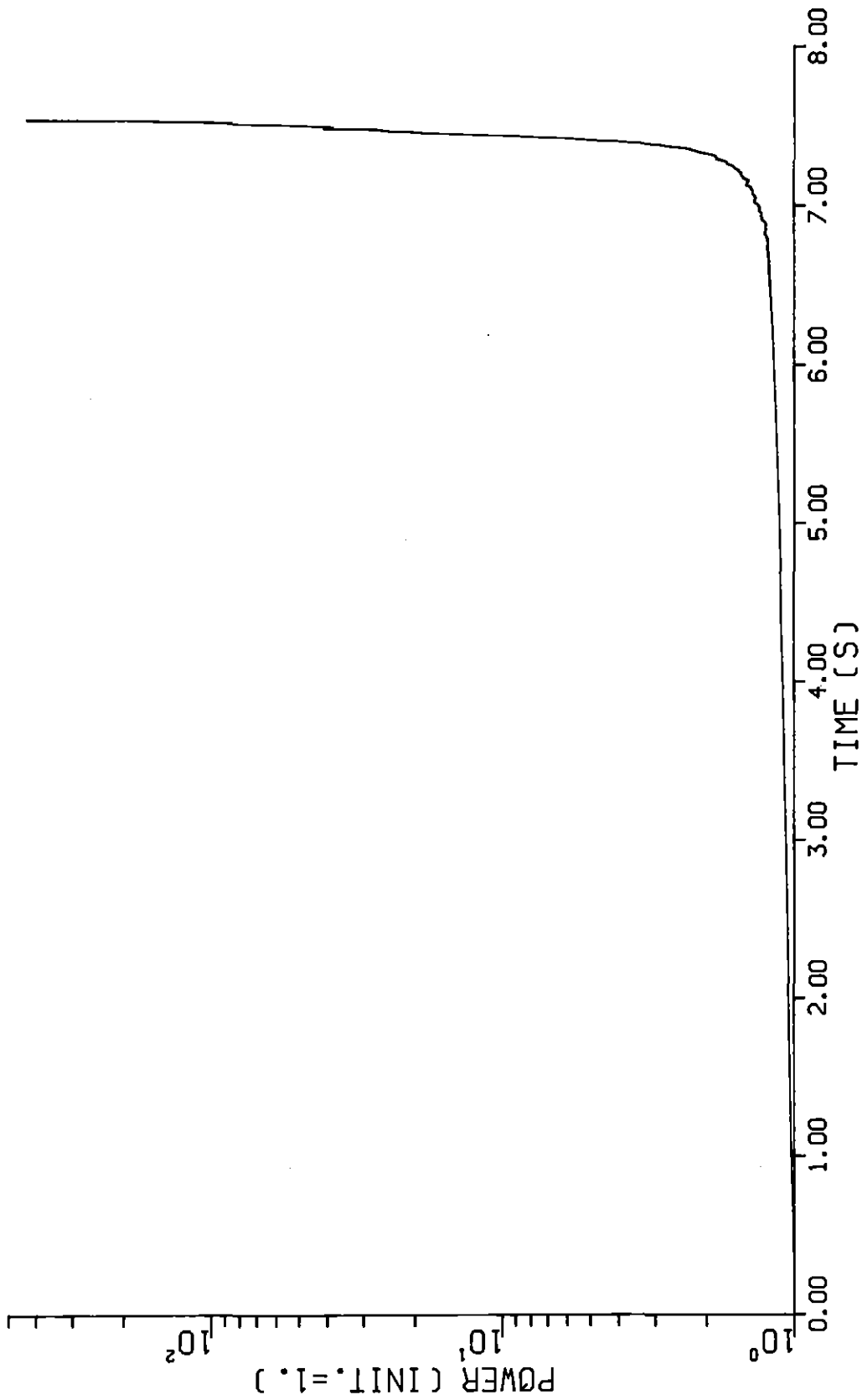


FIG. 6: TIME DEPENDENT POWER (2D)

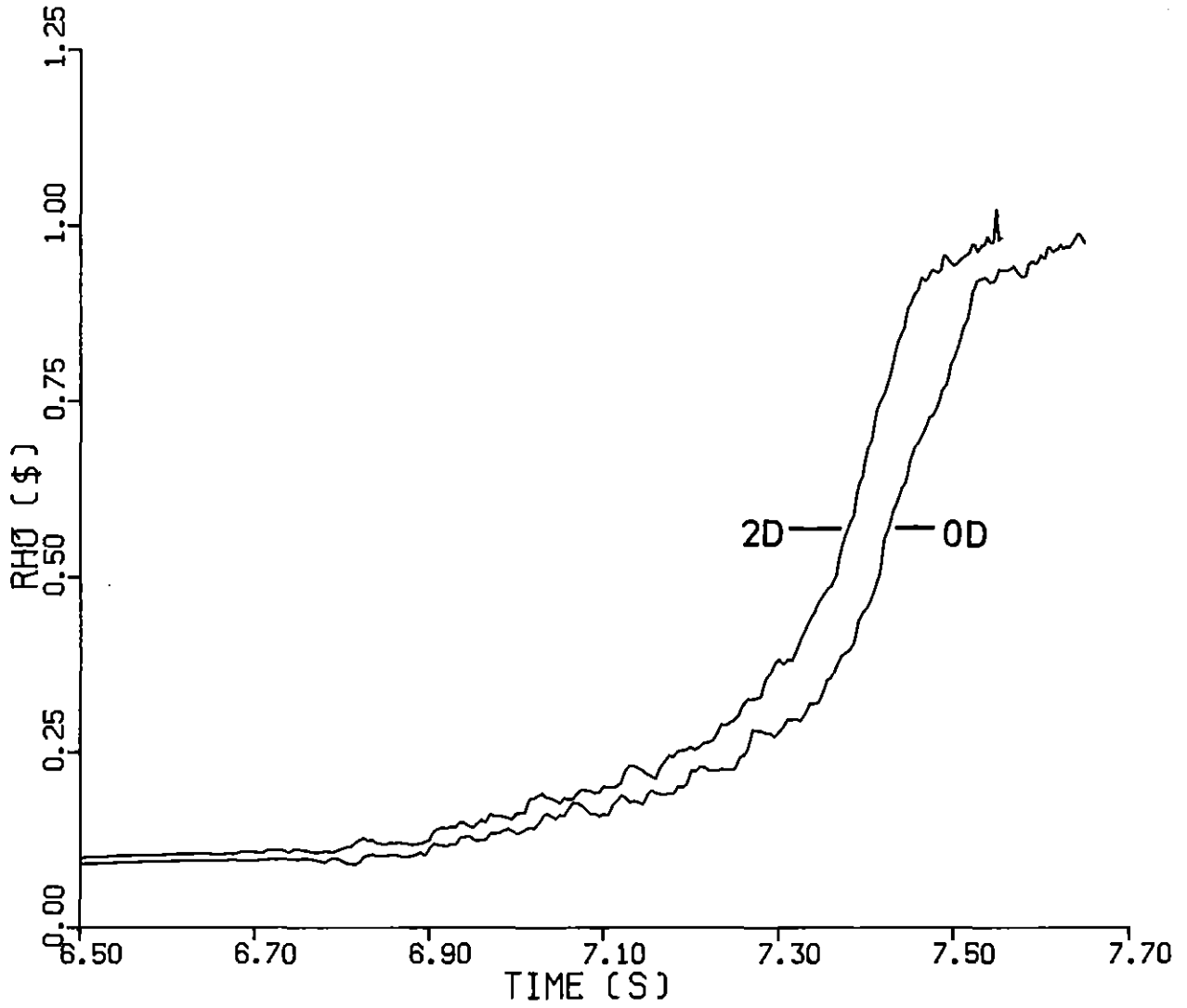


FIG. 7: RHO AFTER ONSET OF VOIDING 2D/0D

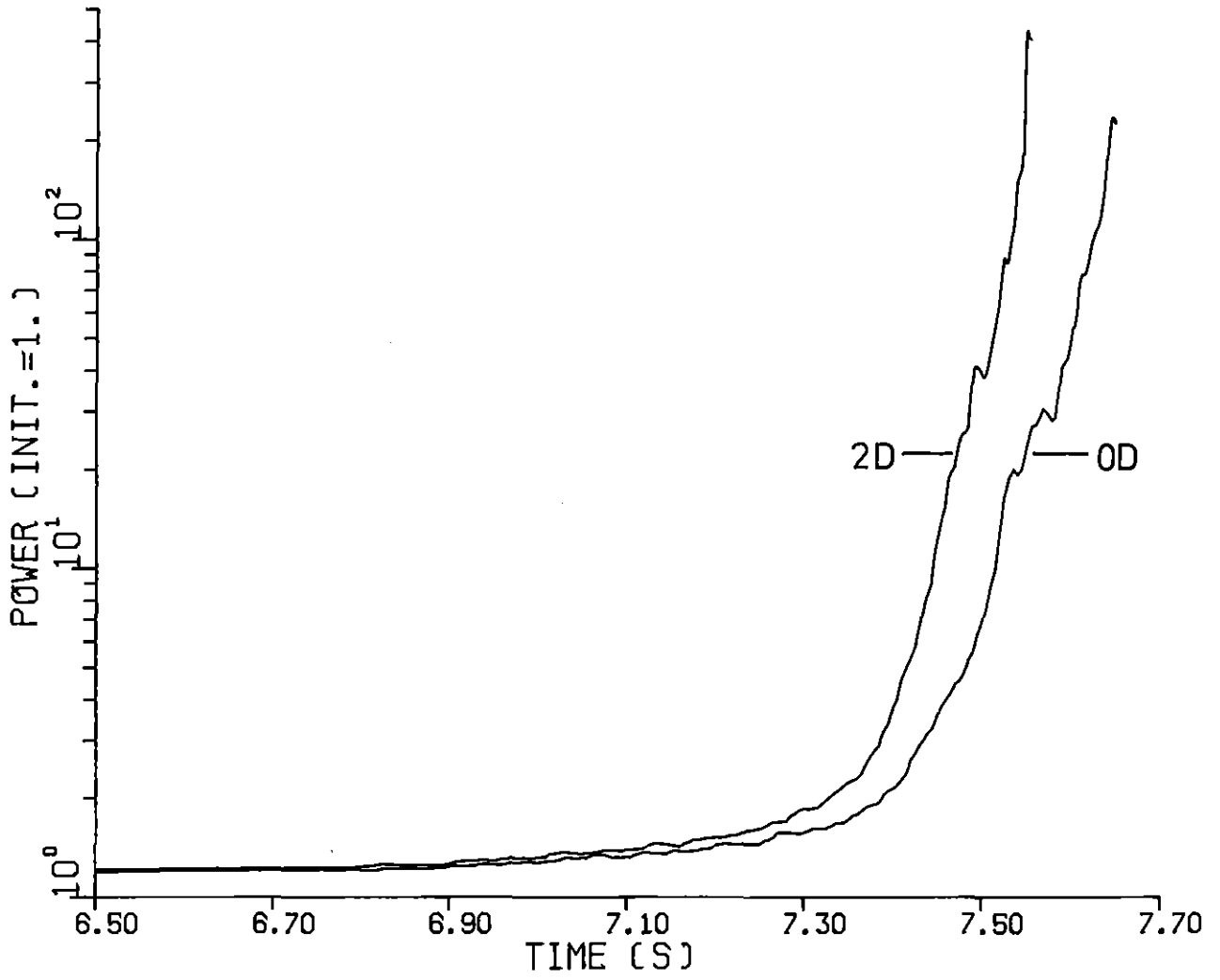


FIG. 8: POWER AFTER ONSET OF VOID. 2D/OD

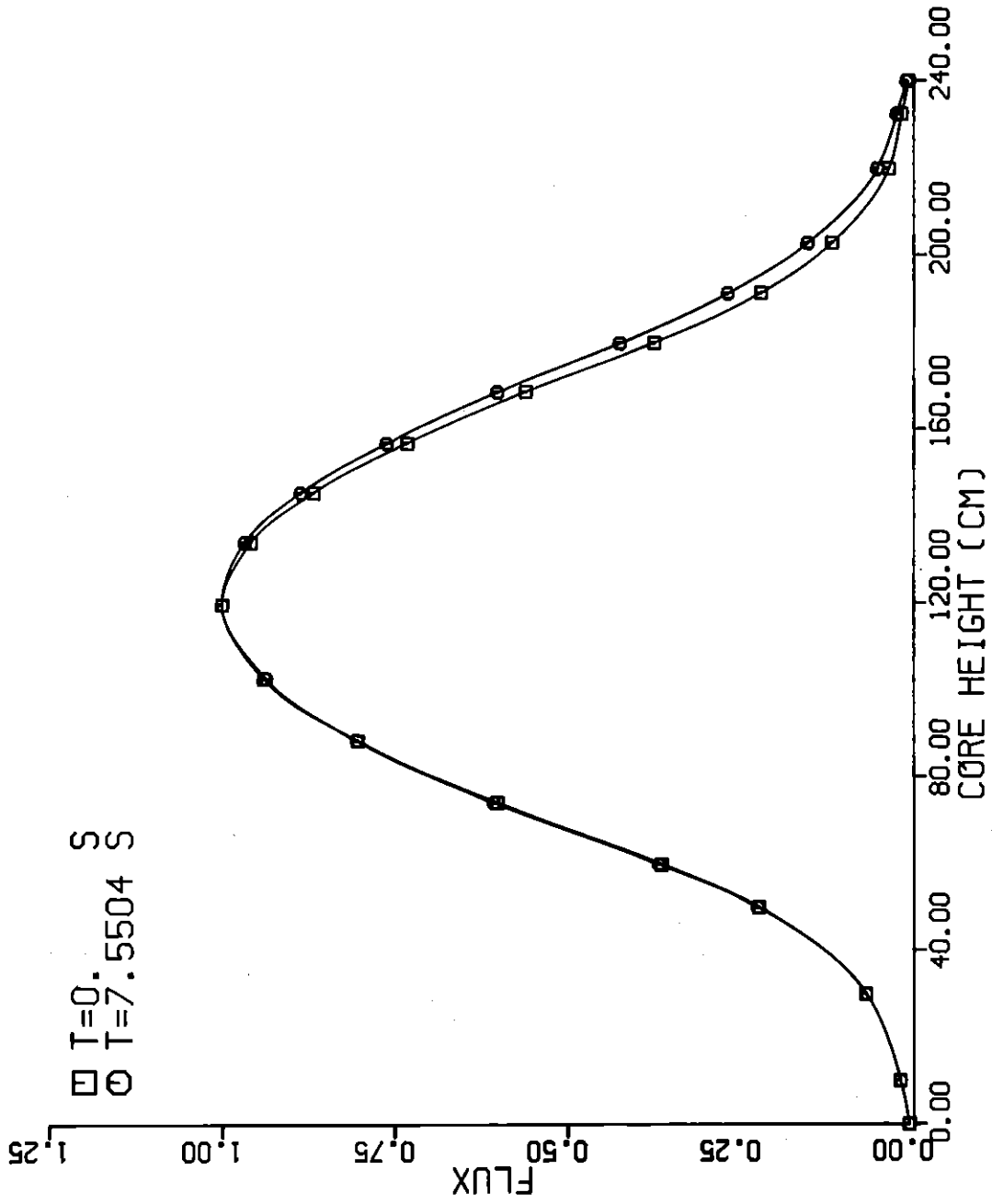


FIG. 9: NORMALIZED AXIAL FLUX, R=24 CM

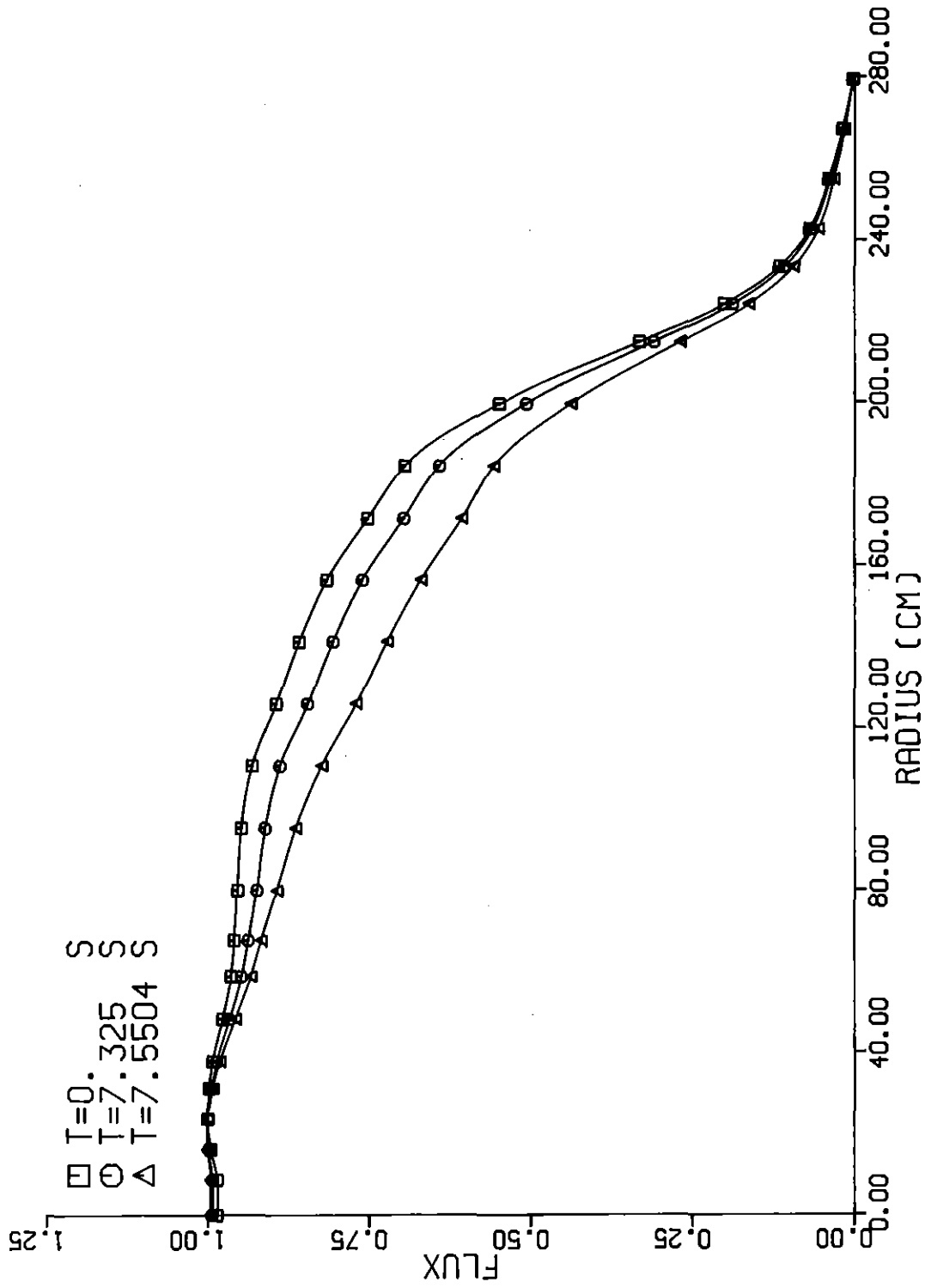


FIG. 10: NORMALIZED RAD. FLUX, H=126 CM

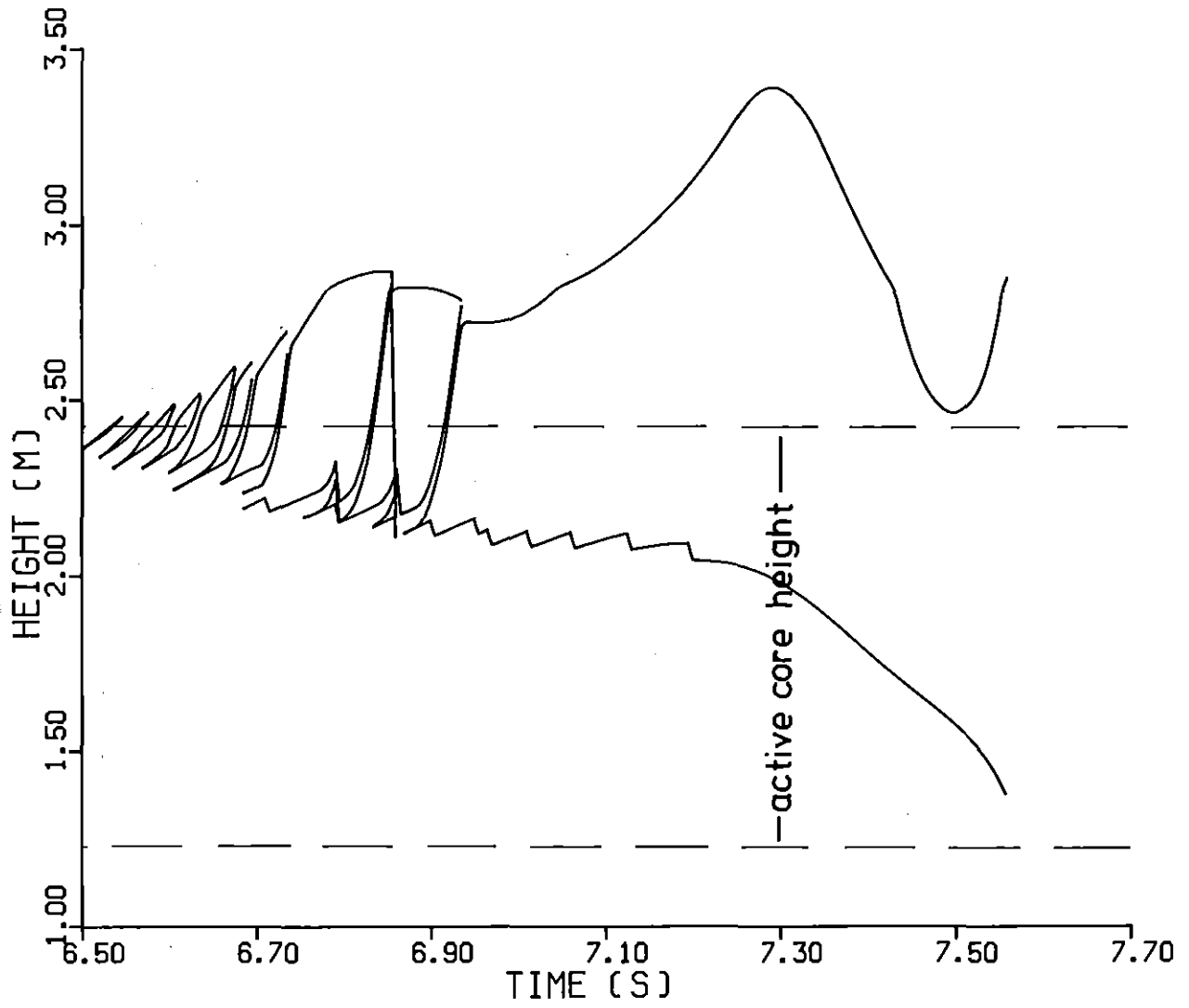


FIG. 11: 2D VOIDING PATTERN CHANNEL 3

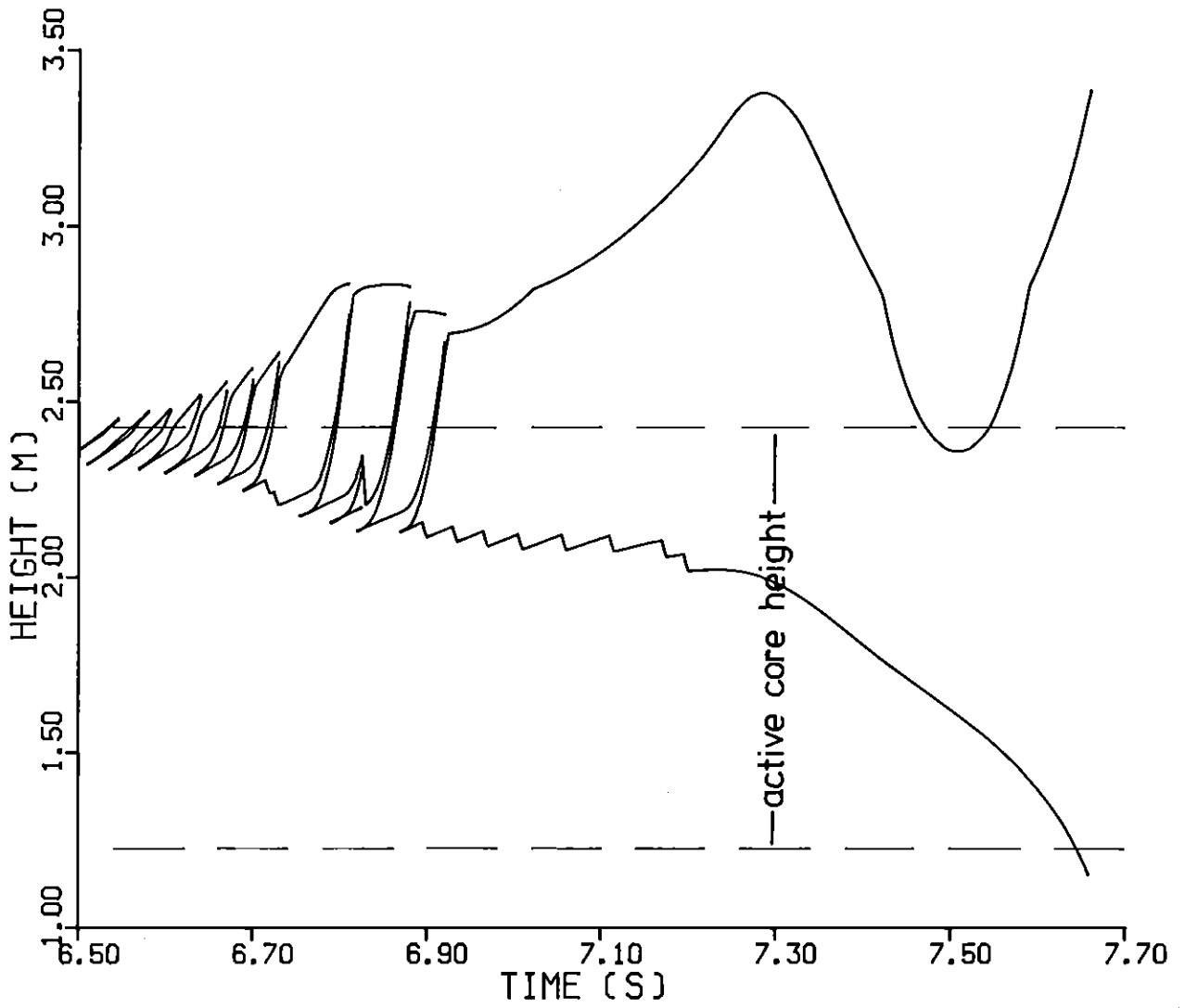


FIG. 12: OD VOIDING PATTERN CHANNEL 3

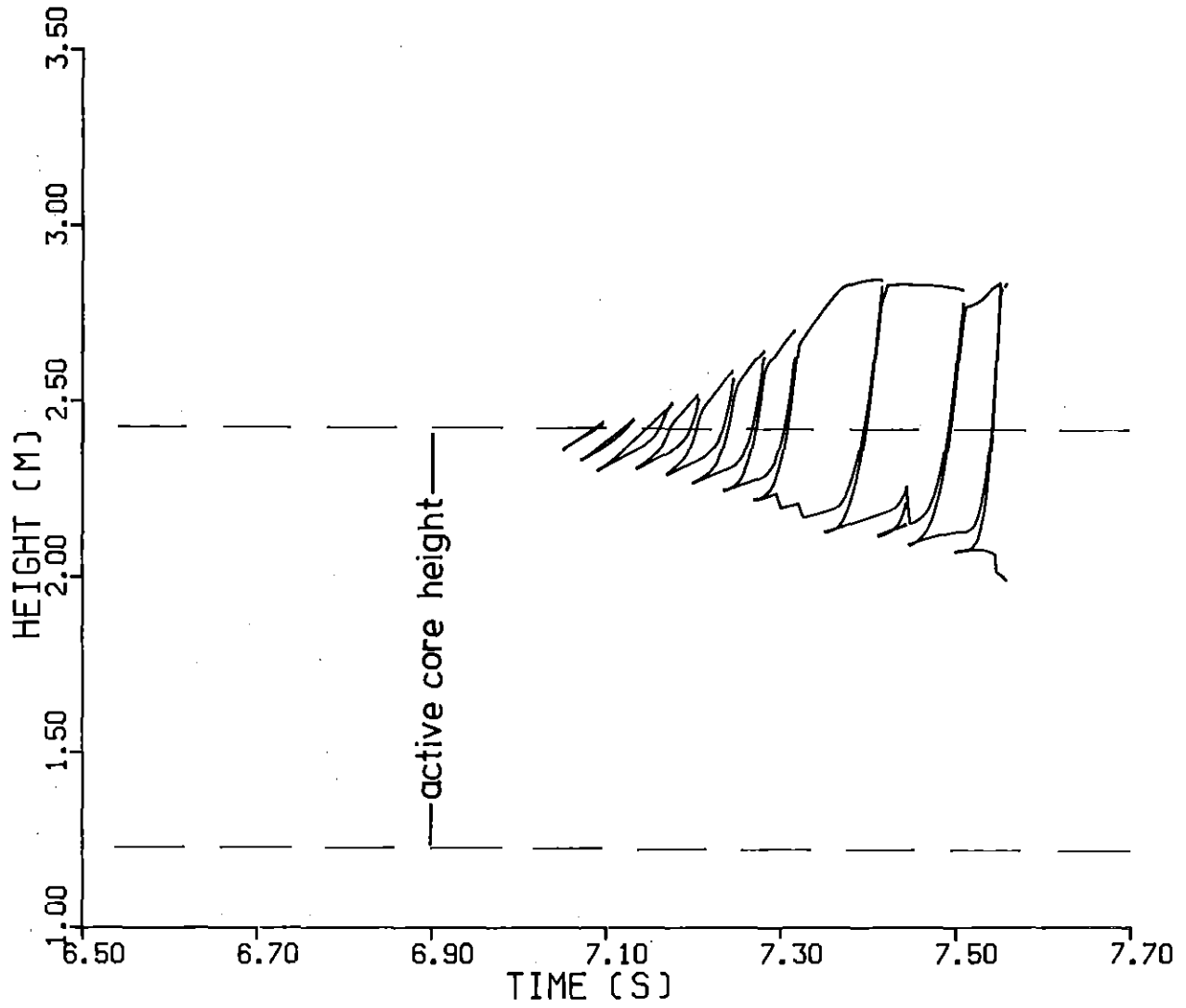


FIG. 13: 2D VOIDING PATTERN CHANNEL 16

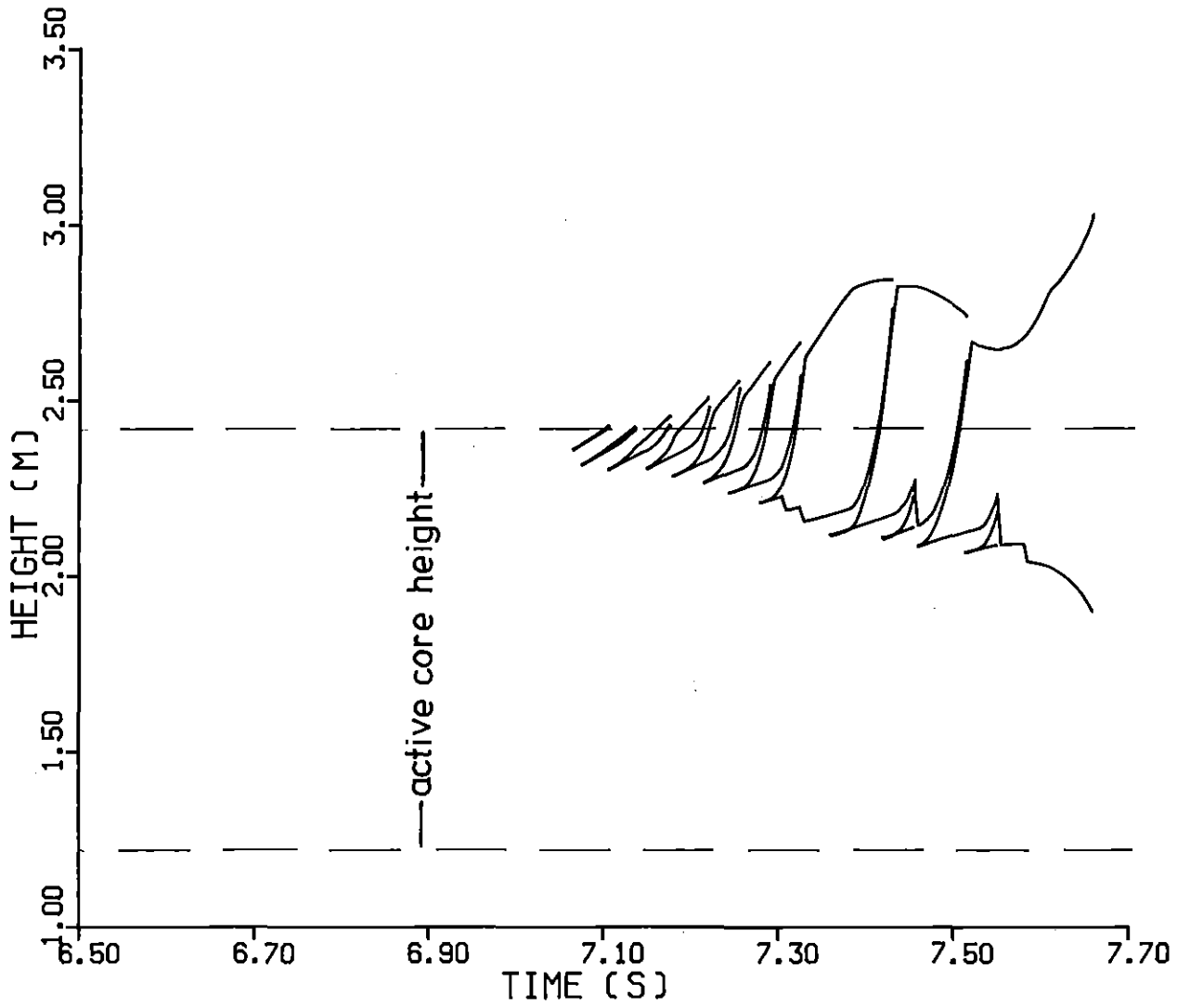


FIG. 14: OD VOIDING PATTERN CHANNEL 16

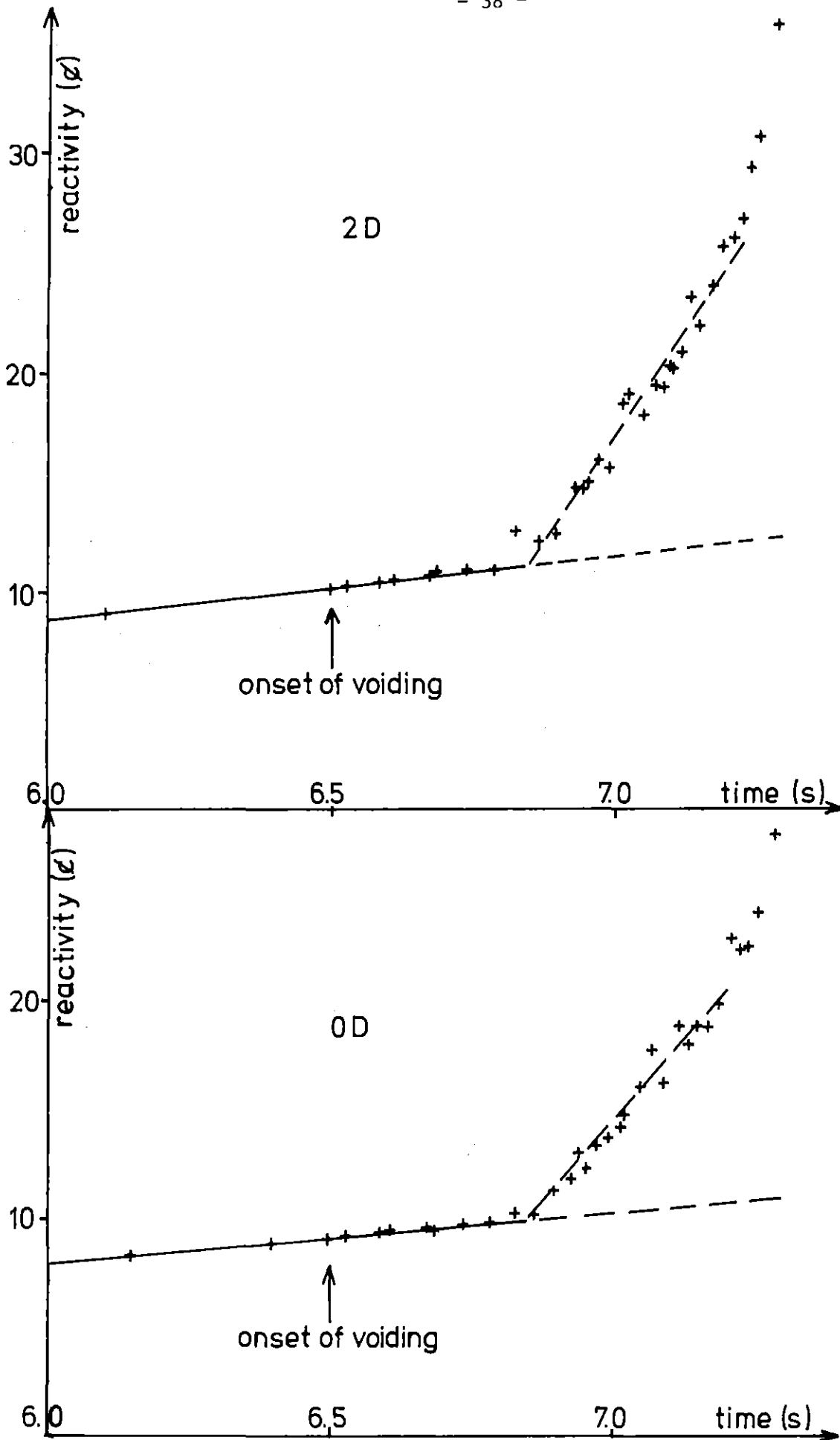


Fig. 15: Time dependent reactivity in the first phase of voiding.

Fig. 16: 2D void distribution at end of prediction at end of predis-assembly.

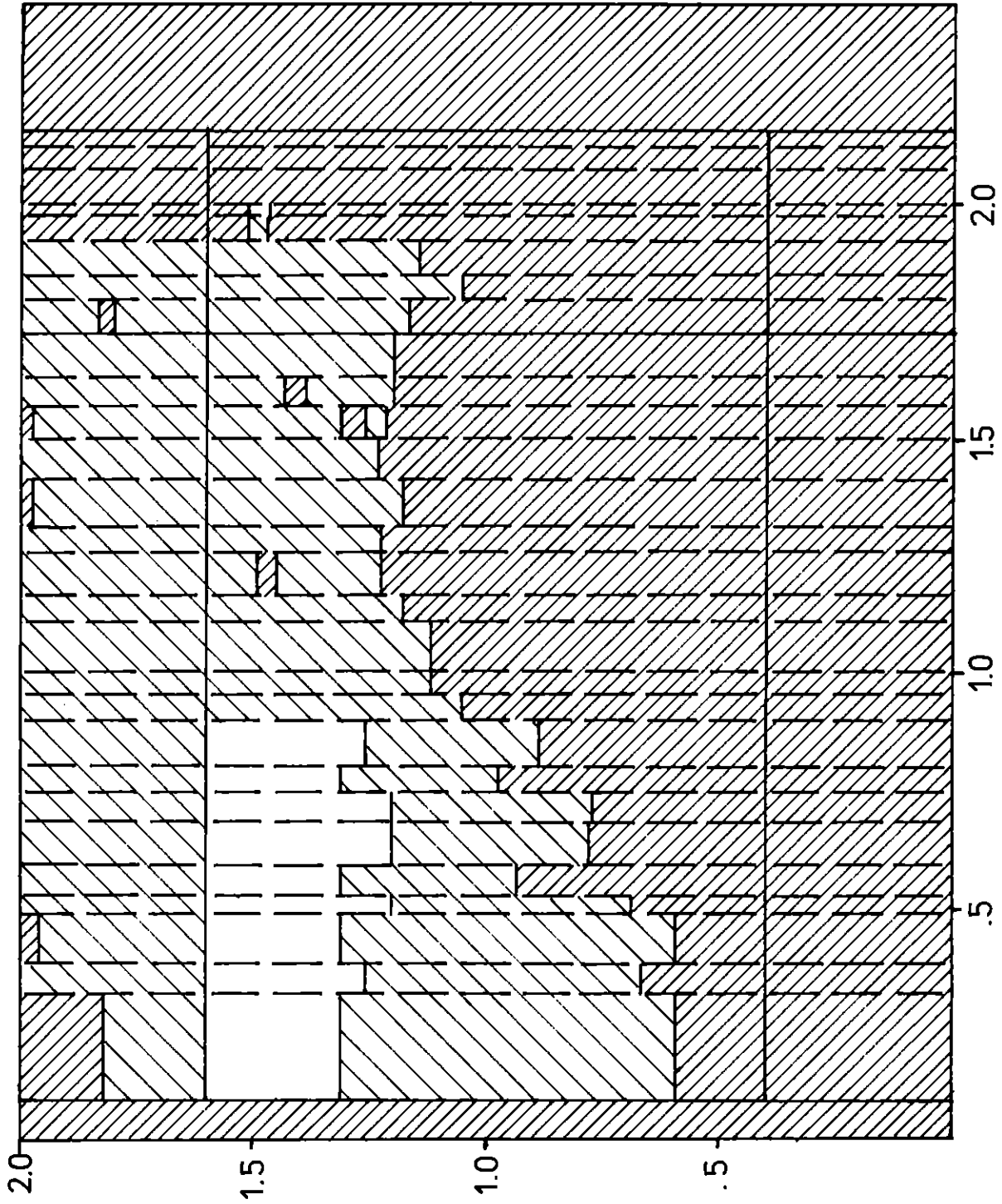
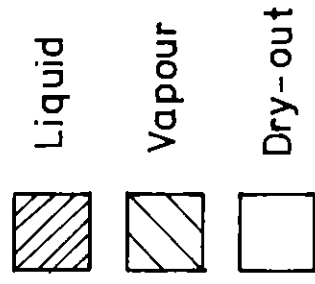


Fig. 17: OD void distribution at end of pre-disassembly

